AIAA 2002-0505
Preliminary Thermal-Mechanical Sizing of Metallic TPS: Process Development and Sensitivity Studies

Carl C. Poteet
Hasan Abu-Khajeel
Su-Yuen Hsu
NASA Langley Research Center
Hampton, VA 23681-2199

40th Aerospace Sciences Meeting & Exhibit
14 - 17 January 2002
Reno, Nevada

For permission to copy or to republish, contact the copyright owner on the first page.
For AIAA-held copyright, write to AIAA Permissions Department,
1801 alexander Bell Drive, Suite 500, Reston, VA, 20191-4344.

PRELIMINARY THERMAL-MECHANICAL SIZING OF METALLIC TPS: PROCESS DEVELOPMENT AND SENSITIVITY STUDIES

Carl C. Poteet*
NASA Langley Research Center, Hampton, Virginia
and
Hasan Abu-Khajeel†, Su-Yuen Hsu†
Lockheed Martin Space Operations, Hampton, Virginia

Abstract

The purpose of this research was to perform sensitivity studies and develop a process to perform thermal and structural analysis and sizing of the latest Metallic Thermal Protection System (TPS) developed at NASA LaRC. Metallic TPS is a key technology for reducing the cost of reusable launch vehicles (RLV), offering the combination of increased durability and competitive weights when compared to other systems. Accurate sizing of metallic TPS requires combined thermal and structural analysis. Initial sensitivity studies were conducted using transient one-dimensional finite element thermal analysis to determine the influence of various TPS and analysis parameters on TPS weight. The thermal analysis model was then used in combination with static deflection and failure mode analysis of the sandwich panel outer surface of the TPS to obtain minimum weight TPS configurations at three vehicle stations on the windward centerline of a representative RLV. The coupled nature of the analysis requires an iterative analysis process, which will be described herein. Findings from the sensitivity analysis are reported, along with TPS designs at the three RLV vehicle stations considered.

Copyright © 2002 by the American Institute of Aeronautics and Astronautics, Inc. No copyright is asserted in the United States under Title 17, U.S. Code. The U.S. Government has a royalty-free license to exercise all rights under the copyright claimed herein for Governmental Purposes. All other rights are reserved by the copyright owner.

*Research Engineer, Metals and Thermal Structures Branch, Structures and Materials Competency
†Aeronautical Engineers, Lockheed Martin Space Operations.

Introduction

Thermal Protection Systems (TPS) on Reusable Launch Vehicles (RLV) are required to be light weight while providing protection from heating during reentry and insulation to cryogenic fuel tanks during ground hold. Recent design goals for RLV have called for "Commercial Aircraft Like" operations, which further increases the importance of the TPS. To meet these goals, TPS must not only be a good insulator capable of withstanding cryogenic and reentry temperatures, but it must be durable and easily maintained. To increase RLV operability, the TPS may be required to withstand exposure to rain and hail.

ARMOR TPS is sized herein to meet the insulation and structural requirements resulting from the groundhold cryogenic environment as well as the ascent and reentry aerothermal heating environments. The analysis focuses on sizing of the fibrous insulation layer and sizing of the honeycomb sandwich on the ARMOR TPS outer surface. Dimensions for other components are based on work reported by Blosser, et al.[3] Insulation layers are sized by the aerothermal heating and cryogenic conditions experienced in the three environments, while the honeycomb sandwich panel on the ARMOR TPS outer surface is sized considering aerodynamic pressure, acoustic pressure, and thermal gradients. Since the thermal performance is dependent on the structure and the structural response is dependent on the temperatures in the TPS, the thermal and structural analyses are coupled, requiring an iterative analysis alternating between thermal and structural analyses.

This paper represents one of several reporting on the development of Adaptable Robust Metallic Operable Reusable (ARMOR) TPS at NASA Langley Research Center.[1-5] ARMOR TPS, as shown in Figure 1, employs a light weight metallic structure to encapsulate high efficiency fibrous insulation and react aerodynamic pressure to the vehicle structure. The goal of ARMOR TPS development is to improve operational features, increase adaptability (by allowing attachment to different tank and structural configurations), and

reduce the weight from previous metallic TPS designs.[2,3] Operability can be increased by modification of TPS design parameters such as outer facesheet gauge (to improve resistance to damage from hail, rain, and orbital debris) and standoff distance from the structure or tank (which greatly improves orbital debris impact resistance[1]).

The final TPS designs reported represent a nominal design which, while exhibiting improved durability and operability compared to previous TPS designs, has not been sized to meet a specific durability or operability criteria, such as a certain size hail, impact energy, or space debris particle size. These criteria are discussed by Dorsey, et al.[2]

ARMOR TPS Design

Figure 1 shows a fabricated ARMOR TPS panel along with a cutaway view showing details of the inner structure. The sandwich panel is exposed to ascent and reentry heating as well as aerodynamic and acoustic pressure. One of the primary functions of the sandwich panel is to re-radiate heat, dramatically reducing the amount of heat absorbed by the TPS. Panel to panel gaps are sealed by overhanging metal foil to prevent ingress of hot gases during reentry. Flutter analysis of these seals is reported by Chen, et al.[4] Pressure loading is reacted to the box beam picture frame through four thermally compliant supports.[3] The supports are arranged in a circular pattern and have low bending stiffness to allow nearly free in-plane thermal expansion of the sandwich panel while resisting translation and rotation. Bulged, compliant sides, made of thin gauge metal foil, form the sides of the TPS panel and block the radiative heat transfer path in the panel to panel gaps. The interior of the TPS panel is filled with Saffil™ high efficiency fibrous insulation.[6] A thin gauge metal foil closes out the bottom of the TPS panel. Several mesh covered vents are incorporated into the metal foil backing to allow the TPS internal pressure to be maintained at local atmospheric pressure.

Selection of materials for ARMOR TPS depends on the maximum surface temperature experienced. For regions of the vehicle where temperatures are under 1100 °F titanium alloys can be used. Regions in excess of 1100 °F use Inconel 617 for the outer honeycomb sandwich panel and compliant sides and Inconel 718 for the thermally compliant supports.

Design of thermal protection systems is dependent on the underlying structure. In this analysis, a single stage to orbit (SSTO) RLV is studied that uses foam-filled-honeycomb-sandwich semi-conformal LOX and LH_2 tanks analyzed in the study by Wang, et al.[7] Figure 2 shows the semi-conformal tanks, where the LOX tank is forward and the LH_2 tank is aft. The intertank structure is not shown. The sandwich panel uses graphite epoxy facesheets with Korex© honeycomb and TEEK[14] cryogenic foam. The cryogenic foam is used to limit heat flow into the tank during groundhold and prevent air liquefaction in the gap between TPS and tank during the vehicle groundhold and ascent conditions. The TPS bottom corners are mechanically attached to a TPS support system (TPSS), which is bonded to the tank wall (Figure 3). TPSS is used to attach TPS to tank structure while accommodating differences in shape between the outer mold line of the vehicle and the tank, and to form a cavity for purging of the system. Purging is performed with gaseous nitrogen during vehicle groundhold to reduce heat flow into the cryogenic fuel tank and to neutralize any potential tank leaks. An air purge after landing is assumed to be a standard operational procedure and is performed using blowers attached 30 minutes after vehicle touchdown to cool the tank and support structure.

Figure 4 is a schematic of the TPSS used in this study, which is composed of two graphite epoxy tabs. The lower tab is bonded to the tank wall and the upper tab is then mechanically attached to the lower tab. A felt layer is bonded to the upper surface of the upper tab. The 3" by 3" area on the upper tab surface is used to attach the corners of four adjacent TPS panels. If necessary, the upper tab can be made out of a higher temperature material to reduce the amount of insulation required.

Analytical Method

Aerothermal Environment and Trajectory

Vehicle loads, aerothermal environment, and trajectory information was obtained from Dorsey, et. al.,[2] for a RLV lifting body configuration designated 3c. This data was used to determine outer surface heating and pressure gradient loads acting on the outer honeycomb sandwich panel. Three vehicle stations were chosen along the windward centerline for analysis: STA 240, STA 802, and STA 1200, where numeric values represent distance from the vehicle nose in inches. Figure 5 shows the location of the vehicle stations relative to the cryogenic fuel tanks. Station 240 is on the LOX tank near the nose of the vehicle. Stations 802 and 1200 are on the LH_2 tank, where STA 802 is near the middle of the RLV and STA 1200 is near the engines. Aerothermal heating rates[2] are shown as a function of time for the three vehicle stations in Figure 6. As can be seen, the heating at STA 240 is significantly higher than the heating at STA 802 and 1200.

Aerothermal heating was calculated using the equation:

$$q = h(H_{rec} - H_g)$$

where h, the heat transfer coefficient, and H_{rec}, the recovery enthalpy, are time dependent quantities obtained from the aerothermal environment data. H_g is the atmospheric gas enthalpy, and is calculated using the empirical equation:

$$H_g = 0.2345 * T + 9.786E-6 * T^2 + \frac{943.6}{T} - 1.57$$

where the units of Hg are Btu/lbm. TPS outer surface temperature is represented by T. Using the recovery enthalpy boundary condition is more accurate than applying a heat flux, since the influence of TPS surface temperature is included.

Thermal Sensitivity Studies

Thermal sensitivity studies were conducted to determine the effect of key assumptions and parameters on TPS insulation requirements and weight. The areas studied were: purging during groundhold, reentry purge initiation time, reentry initial temperature, and TPSS temperature limit. A one-dimensional transient heat transfer finite element model, including elements to model the effects of heat shorts, was created for use in the sensitivity studies and for later use in the sizing analysis. Studies by Blosser have shown that one dimensional models reasonably predict temperatures in TPS systems.[8]

Thermal Finite Element Model

Figure 7 shows a diagram of the thermal finite element model of the TPS/TPSS/Tank system. The TPS/TPSS/Tank system is shown schematically in Figure 3. In the model diagram, surfaces are depicted by open circles, and were used to apply boundary conditions and keep track of surface related quantities, such as coating emissivity and surface area. Nodes are represented by filled circles, and rod heat transfer elements are represented by lines.

The honeycomb sandwich on the TPS outer surface was modeled using three rod heat transfer elements in parallel, along with increased thermal capacitance at the end nodes to account for facesheet thermal mass. The three elements were used to model solid conduction through the core, gas conduction in the enclosed honeycomb, and radiative heat transfer between the outer and inner facesheets and the core, respectively. The gas thermal conductivity was determined using[9]:

$$k_g = \frac{k_g^*}{1 + 2\left(\frac{2-\alpha}{\alpha}\right)\left(\frac{2\gamma}{\gamma+1}\right)\left(\frac{1}{\mathrm{Pr}}\right)\left(\frac{\lambda}{L_c}\right)}$$

where k_g^* is the temperature-dependent gas thermal conductivity for air, α is the accommodation coefficient, γ is the specific heat ratio for air, and Pr is the Prandtl number. L_c is the characteristic length of the enclosure. In this work, the characteristic length was assumed to be the core height. The mean free path, λ, is given by:

$$\lambda = \frac{K_B T}{\sqrt{2}\pi d_g^2 P}$$

where K_B is the Boltzmann constant, d_g the gas collision diameter, and T and P the temperature and pressure, respectively. Radiation inside honeycomb core was approximated using a rod element with an equivalent conductivity calculated using the equations developed by Swann and Pittman[10]:

$$k_{rad} = 4\zeta\sigma T_{avg}^3 L$$

where T_{avg} is the average rod element nodal temperature, σ is the Stefan-Boltzmann constant, L is the honeycomb core height, and ζ is given by:

$$\zeta = 0.664(\beta + 0.3)^{(-0.69)} \varepsilon^{1.63(\beta+1)^{(-0.89)}}$$

In this equation, ε is a uniform emissivity value inside the honeycomb and β is given by:

$$\beta = \frac{L}{d}$$

where d is the honeycomb cell size.

The primary mode of heat transfer through the TPS will be through the Saffil fibrous insulation layer, due to its large area. Saffil thermal conductivity is highly pressure dependent, so it was necessary to model both temperature and pressure dependency of the insulation layer material properties.

In addition to heat transfer through the insulation, the heat shorts resulting from the compliant sides and thermally compliant supports were also included, as well as a model of the box beam on the lower surface of the TPS that included four elements in parallel to simulate solid conduction through the box beam sides,

solid conduction through the mechanical fasteners, gas conduction, and radiation.

The TPS panel rests on a Nomex felt pad at each corner and is mechanically fastened to the TPSS. The TPSS was modeled with two solid conduction elements, one representing the Nomex pad and the other representing mechanical fasteners. A cavity is formed between the back of the TPS panel and the outer surface of the tank. Heat transfer across the cavity was modeled with two elements in parallel, one modeling gas conduction in an enclosure and the other modeling radiation between infinite parallel plates. Finally, the foam filled honeycomb sandwich tank structure was modeled with four elements in series, representing solid conduction through the cryogenic foam and honeycomb core. The thermal capacitance of the end nodes was increased to account for facesheet thermal mass.

Thermal Load Cases

The boundary conditions were varied to represent the thermal conditions expected during the RLV flight cycle. Three transient thermal loadcases were defined: groundhold, ascent, and reentry.

Groundhold analysis assumed the cavity between the back of the TPS panel and the outer surface of the sandwich tank to be purged with gaseous nitrogen. This was simulated by applying convection boundary conditions to the surfaces marked "Purge BCs" in Figure 7. Purge temperature was assumed to be -160 °F. A heat transfer coefficient of 1.0E-3 Btu/s-ft-R was used to represent forced convection heat transfer, based on the work reported in Reference 11. Based on empirical calculations, this corresponds to a flow rate on the order of 3 ft/s. The purge boundary condition drives the node at which it is applied to within a few degrees of the purge gas temperature, effectively acting like a prescribed temperature boundary condition, so that increasing flow rate beyond 3 ft/s will not significantly influence the results. A prescribed temperature boundary condition is applied to the surface marked "Inner Surface BC" to model the effect of cryogenic fuel, where temperatures of –423 and –300 °F were used for the LH_2 and LOX tank, respectively. In addition, a convective boundary condition, with heat transfer coefficient of 6.94E-4 Btu/s-ft-R is applied to the surface "Outer Surface BC", allowing convection to ambient air at 70 °F. The heat transfer coefficient is obtained from Reference 13 and represents typical launch pad conditions.

In the ascent loadcase the purge boundary condition was removed. The same cryogenic boundary condition on "Inner Surface BC" used in the groundhold loadcase was used in the ascent loadcase. Finally aerothermal heating and radiation to space boundary conditions are applied on the surface labeled "Outer Surface BC". Data for calculation of aerothermal heating on the TPS outer surface was obtained from the RLV 3c ascent aerothermal data file.[2] Radiation to space was modeled assuming an emissivity of 0.86 and 0.8 for TPS with an Inconel 617 and titanium outer honeycomb sandwich panel, respectively.

The reentry loadcase applied aerothermal heating and radiation to space boundary conditions on the "Outer Surface BC" surface. All other surfaces were adiabatic. As with the ascent loadcase, emissivities of 0.86 and 0.8 are assumed for TPS with Inconel 617 and titanium outer honeycomb sandwich panels, respectively. It takes approximately 43 minutes for the RLV to touch down, however peak temperatures in the tank wall often occur after touch down. For this reason, it is necessary to extend analysis to simulate the vehicle sitting on the runway. At 43 minutes the boundary condition applied to "Outer Surface BC" is changed from aerothermal heating and radiation to a convection boundary condition with air temperature set at 70 °F. It was assumed that an air purge is initiated in the cavity region 30 minutes after touchdown in order to cool down the TPS and tank, with 30 minutes being an estimate of a reasonable amount of time to hook up ground based blowers to the RLV. Since the purge is performed in the area of the TPS / tank system that will be most sensitive to over-heating, i.e. the TPSS and the tank wall, it is assumed that the purge works very quickly to reduce temperatures. The analysis is therefore concluded at the initiation of purging. Sensitivity studies were performed to assess the benefits of performing reentry purging more quickly after touchdown, or even while the RLV was traveling at subsonic speeds via an air scoop, and will be reported in the results section.

Insulation Sizing Criteria

Both the Saffil insulation thickness and the foam filled honeycomb core thickness were sized using iterative thermal analyses, increasing or decreasing layer thicknesses until an optimum solution was reached. Saffil insulation thickness was minimized with constraints that temperature limits in the TPS, TPSS, and tank were not exceeded during ascent or reentry loadcases, resulting in at least one critical node with temperature equal to a temperature constraint (within a +/- 5 °F tolerance). The foam filled honeycomb thickness was optimized such that heat flux into the cryogenic fuel was under 0.01 Btu/s-ft^2 and air liquefaction was prevented during groundhold and ascent. The heat flux constraint is based on conservative estimates of heat flux into the shuttle external fuel tank reported in Reference 11. A pressure

dependent relation was used for air liquefaction to allow accurate determination of air liquefaction conditions during ascent. This can become an important consideration when purging is performed during groundhold.[11] A final constraint was placed on the foam filled honeycomb that the minimum thickness equal the thickness of the tank as determined by structural sizing.[7]

Loads Table Generation

To perform combined thermal and structural analysis and sizing, a loads table was needed after each thermal analysis to allow determination of cases to be structurally analyzed. A representative loads table is shown in Table I for STA 1200. The loads table is used to collect thermal analysis, aerothermal environment, and trajectory data for several different structural load cases. Load cases were defined for both ascent and reentry. Ascent cases were liftoff, maximum normal force, maximum pressure gradient, maximum thermal gradient, and maximum axial acceleration. Reentry cases were maximum thermal gradient, maximum surface heat flux, and maximum pressure gradient. Data collected for each case includes temperatures, atmospheric pressure, static normal pressure acting on the TPS surface, and vehicle accelerations. Acoustic pressure is calculated based on dynamic pressure, as described in Reference 2.

Pressure gradient acting on the TPS outer honeycomb sandwich panel was determined using the equation:

$$\Delta p_{ultimate,TPS+} = 1.4\left(\Delta p_{aerodynamic} + 3\Delta p_{rms,acoustic}\right)$$

$$\Delta p_{ultimate,TPS-} = 1.4\left(\Delta p_{aerodynamic} - 3\Delta p_{rms,acoustic}\right)$$

where $\Delta P_{ultimate,TPS+}$ and $\Delta P_{ultimate,TPS-}$ represent the maximum inward and outward pressure expected from the combination of aerodynamic pressure and three standard deviations of acoustic pressure, acting in either the positive or negative direction. A factor of safety of 1.4 is applied to the loads.

The ARMOR TPS design forms an aerodynamic shell that carries aerodynamic pressure on the TPS outer surface. The inside of the TPS panel is vented to local atmospheric pressure. In reality there may be variations between TPS internal pressure and local atmospheric pressure due to a pressure lag effect, however data on this effect was not available, and the assumption that TPS internal pressure equals local atmospheric pressure was deemed adequate for preliminary sizing of TPS. This allows calculation of ΔP_{aero} using the formula:

$$\Delta p_{aerodynamic} = p_{local\_static} - p_{atmospheric}$$

where P_{local_static} is the inward acting component of local aerodynamic pressure and $P_{atmospheric}$ is the local atmospheric pressure at the current vehicle altitude. A positive value indicates inward acting pressure.

Structural Model

A structural finite element model was used to calculate deflection of the outer honeycomb sandwich panel and consisted of: outer honeycomb sandwich panel modeled with composite shell elements, thermally compliant supports modeled with bar elements, and box beam frame modeled with bar elements. Figure 8 shows the resulting finite element model. Uniform pressure loading was applied on the sandwich outer surface, and temperatures were applied over the entire model. Loads were obtained from the loads table at specific times of interest.

Degraded material properties were used for Inconel 617 foil facesheets to account for the effect of brazing in the fabrication process. In addition, temperature dependent properties were used for Inconel 617 and Ti 1100.

The model was constrained at points A, B, C, and D as shown in Figure 8. All points were allowed z rotational freedom. All other degrees of freedom at Point A were fixed. Points B and C both had z rotational freedom, in addition point B had translational freedom in the x direction and point C had translation freedom in the y direction. Point D was given translational freedom in the x and y direction as well as z rotational freedom. All other degrees of freedom at points B, C, and D were fixed. The boundary conditions represent mechanical attachment to expansion slots, as described in Reference 3. Figure 9 shows a representative deflection (plot of z displacement) resulting from an inward acting (positive) pressure.

Iterative Sizing Method

Thermal-mechanical sizing of the TPS panel was performed following the logic shown in Figure 10. The process consists of the following steps: Making an initial guess of design parameters, performing iterative transient thermal analyses to size insulation layers, creating a loads table from thermal analysis results and vehicle data, static deflection analysis of the outer honeycomb sandwich, and finally local failure analysis of the outer honeycomb sandwich. There are two

primary sizing loops in the process: an inner loop occurs in the structural sizing of the honeycomb sandwich to determine the minimum weight design that satisfies both deflection and local failure criteria, the outer loop is used for convergence of the structural parameter values guessed in the thermal analysis with those obtained through structural analysis. This process has to be repeated for each vehicle station analyzed. Three windward centerline vehicle stations (STA) were selected for analysis: STA 240, STA 802 and STA 1200, where the numerical value is the station location in inches from the nose of the RLV. STA 240 was selected because it is near the nose and experiences significant entry heating, STA 802 is roughly half the vehicle length from the nose and is representative of the vehicle windward acreage area, and STA 1200 is located near the engines, where high acoustic loading occurs during ascent.

Several structural components were sized in a companion study[3]: thermally compliant supports, box beam, and TPS support structure. It was possible to size these components independently from the present activity. In addition, the tank structure was optimized in the work by Wang, et. al.[7]

In order to start the sizing process shown in Figure 10, an initial guess of insulation and structural parameter values is made based on previous experience analyzing TPS. Thermal analysis and sizing of insulation thickness is then performed using the thermal finite element model, as previously described.

Next, a loads table is generated. The loads table is used to collect thermal analysis, aerothermal, and trajectory data for several different structural load cases. Critical load cases were determined from the loads table for structural analysis and sizing. Linear static deflection analysis of the honeycomb panel due to thermal and pressure gradients was performed with NASTRAN. Deflection limits were imposed to prevent boundary layer transition at high Mach numbers and to prevent permanent compaction of fibrous insulation. Excessive deflection of the TPS outer surface can result in an early transition of flow type from laminar to turbulent. For this reason, at velocities greater than Mach 5.0, a deflection limit based on Table II is imposed on the honeycomb sandwich panel.[2] In Table II, L is the diagonal length of the TPS panel. The second deflection limit, imposed to prevent permanent insulation compaction, is in effect for all loadcases, and requires that the TPS outer sandwich panel deflection not exceed 10% of the total TPS panel thickness.

Two different materials were considered for the outer honeycomb sandwich: Inconel 617 and Ti 1100. Material selection was based on maximum temperature reached and time at that temperature. A range of facesheet thickness (0.006" to 0.016" in increments of 0.001") and honeycomb depth (0.25" to 1.00" in increments of 0.05") was considered. The 0.006" facesheet thickness represents minimum facesheet gauge for the materials considered, and is based on manufacturing considerations. It may be necessary to increase the minimum gauge in the future to account for criteria such as ground hail, flying through rain, etc., as described in Reference 2. Also, four different honeycomb specifications (ribbon thickness x cell size) were considered: 0.002"x1/8", 0.002"x3/16", 0.002" x1/4", and 0.002"x3/8". A routine was created to automatically analyze and determine the weight of all honeycomb designs, a total of 704 designs, in the design space defined by the sandwich panel variables. From this, a table of candidate designs, sorted by increasing weight, was created for each material (Inconel 617 and Ti 1100).

The lowest weight honeycomb sandwich panel that passed deflection criteria was then analyzed to check for localized failures. Local honeycomb stress failure criteria were checked using Hypersizer®[12] and included: in-plane tensile failure and in-plane shear failure of the facesheets, intracellular dimpling of the face sheets, transverse shear failure of the core, and core crushing. At this point, the first decision box in Figure 10 has been reached. If the candidate honeycomb sandwich passes the localized failure criteria, analysis proceeds to the second decision box. Otherwise, the next heavier honeycomb sandwich that passed the deflection criteria is selected and checked for localized failure. This inner loop is repeated until a design is found that passes.

The second decision box, shown in Figure 10, compares the structural parameters used in the thermal analysis to the structural parameters determined from the structural analysis. If the parameters are within tolerance, the analysis for this vehicle station is complete. Otherwise, it is necessary to return to thermal analysis with the updated structural parameters. Tolerance was defined as +/-0.002" for facesheet gauge and +/-0.05" for honeycomb depth. In all cases honeycomb gauge and honeycomb cell size was matched exactly between thermal and structural analysis.

Results

Thermal Sensitivity Study

Thermal sensitivity studies were performed to examine the effect of:

1. Groundhold purging on system weight
2. Earlier reentry purging
3. Assumed initial reentry temperature

4. Increasing TPSS temperature limit

Structural parameters were held constant throughout this study, with emphasis on determining the influence of the stated changes on Saffil and cryogenic foam filled honeycomb layer weight.

Weights directly related to insulation layer thickness (Saffil, cryogenic foam insulation, compliant supports and sides, and cryogenic fuel tank honeycomb core) were calculated for typical TPS designs and compared to the overall weight of the TPS, TPSS, and tank sandwich panel. As can be seen in Figure 11, the weight directly related to insulation layer thickness amounts to between 34% and 39% of the overall TPS / tank system weight, depending on which vehicle station is examined.

Figure 12 compares insulation weight of systems that were purged during groundhold with unpurged systems. At STA 240 and STA 1200 purging had no effect on system weight. This is due to the constraint that cryogenic foam insulation thickness be greater than or equal to the core thickness determined by structural analysis of the tank. At STA 802 purging resulted in an increase in required cryogenic foam thickness to prevent violation of the constraint limiting heat flux into the tank. Insulation requirements can be reduced at this vehicle station by reducing the purge temperature.

Most analyses assumed that a reentry purge was performed 30 minutes after vehicle touchdown, which would be accomplished by attaching external blowers to the RLV to vent the cavity between TPS and tank. In Figure 13, the effect of purging at an earlier time is examined. Times of 4365 and 3465 seconds correspond to 30 and 15 minutes after touchdown, respectively. Purging at 2360 seconds represents purging while the RLV is still in the air at subsonic velocity via an air scoop. As can be seen there is only a small benefit to purging earlier. However, if purging could be initiated at supersonic velocities it is likely that there would be a significant weight savings.

In reentry vehicle insulation sizing the initial temperatures of the TPS and tank are uncertain parameters. These parameters are determined by the specific operation of the vehicle prior to reentry, and are not known at a preliminary design stage. Figure 14 shows that there is significant sensitivity of TPS insulation related weights to assumed initial temperature. This information may be useful from an operations standpoint, since it indicates that measures taken on orbit to reduce vehicle temperature prior to reentry will significantly reduce TPS weight. It is interesting to note that there is a large jump in insulation related weight between assumed initial reentry temperatures of 70 and 250 °F. This results from the fact that reentry insulation sizing is being driven by the 300 °F temperature limit of the TPSS and tank structure. By increasing the initial temperature from 70 to 250 °F, the allowed change in temperature of the TPSS and tank is reduced from 230 °F to 50 °F, which means that the heat capacity of the TPSS and tank that can be used to store the absorbed energy during reentry is reduced by a factor of 4.6.

The TPSS and cryogenic fuel tank facesheets were assumed to be made of graphite epoxy with a maximum temperature limit of 300 °F. In all analyses, the TPSS temperature limit constraint was active in the sizing of Saffil insulation. It was anticipated that using a material with a higher temperature limit for the TPSS would significantly reduce TPS weight. For this final sensitivity study, the temperature limit of the TPSS was increased to 350 °F, which resulted in the tank structure temperature limit becoming the active constraint during Saffil insulation sizing. Since the tank structure temperature limit constraint was already close to being active, only a small weight reduction was seen at STA 240 and STA 1200, with a larger 12% weight reduction at STA 802. From these results, it appears that to significantly reduce TPS weight, both the TPSS and tank temperature limits need to be increased.

Thermal-Mechanical TPS Sizing

TPS panel sizing required iteration between thermal analysis and structural analysis. The results reported are for the final, converged solution.

Table III shows the results of thermal sizing of the insulation layers at three vehicle stations. Maximum TPS surface temperatures ranged from 1514 °F at STA 240 to 1140 °F at STA 1200. Inconel 617 TPS was used for STA 240 since the maximum surface temperature is well above the temperature limit of Ti 1100. Two cases were examined at STA 802. Case number 2 used Inconel 617 TPS and case number 3 used Ti 1100 TPS. This was done to assess the potential benefits of running Ti 1100 past the material temperature limit. At STA 1200 Ti 1100 TPS was used, since the maximum surface temperature is close to the temperature limit of Ti 1100. Reentry insulation ranged from 1.89" to 3.08", with all cases being sized by the TPSS temperature limit. Cryogenic insulation thickness ranged from 0.62" to 0.82"; with sizing driven by either allowable heat flux into the fuel tank during groundhold or minimum structural thickness of the fuel tank sandwich panel.

Table IV shows results from structural sizing of the TPS panel honeycomb sandwich panel. In all cases, honeycomb core was selected with 0.25" cell size and 0.002" ribbon gauge. Honeycomb thickness ranged from 0.30" to 0.75", depending on vehicle station and material used. Facesheet thickness was normally sized

by the minimum material gauge constraint of 0.006", but was 0.008" at STA 1200.

The "Sizing Information" section of Table IV reports the loadcases that produced the worst loading conditions for sizing of the honeycomb panel due to deflection and local failure modes. "Critical Deflection Loadcase" identifies the loadcase that resulted in the maximum honeycomb panel deflection. "Critical Local Failure Loadcase" reports the loadcase that produced the lowest margins of safety used in sizing for localized failure modes. Finally, the "Critical Local Failure Mode" lists the local failure mode with the lowest margin of safety.

Examining the results for STA 240 in Table IV, it can be seen that both the critical deflection and local failure loadcase was the maximum pressure gradient case during ascent, where the pressure gradient acting on the outer TPS surface is 1.76 psia. This loadcase occurs 60 seconds after liftoff.

Cases 2 and 3 were performed at STA 802, with Inconel 617 honeycomb sandwich panel used in Case 2 and Ti 1100 honeycomb sandwich panel used in Case 3. In both cases, the critical deflection and local failure loadcase was due to engine acoustic pressure during the initial seconds of liftoff. Pressure gradient on the outer surface was 1.3 psia, primarily due to engine acoustics. A thicker honeycomb sandwich was required when titanium was used. However, as will be seen, the titanium sandwich was still significantly lighter than the Inconel 617 sandwich.

Vehicle station 1200 required the thickest outer honeycomb core, 0.75". Structural design at this station is interesting in that initial sizing iterations were driven by liftoff acoustics, resulting in increased honeycomb core thickness. However, as the honeycomb core was made thicker thermal gradients through the core became more significant to panel deflection, until the reentry maximum thermal gradient loadcase became the structural sizing driver. This loadcase occurs 38 minutes into reentry, shortly before touchdown. The thermal gradient is –356 F (resulting in inward concaved panel shape) with minimal aerodynamic pressure. The critical loadcase for localized failure sizing was still the liftoff condition, due to the 4.26 psia pressure gradient, predominantly due to engine acoustics.

Table V shows a representative TPS weights calculation at STA 1200. The table includes assumptions for material properties and design parameters on the left hand side and a weights breakdown by component on the right hand side. It is assumed that the honeycomb core and skin are joined using a Liquid Interface Dispersion (LID) technique with properties as listed. Properties for Ti 1100 were obtained from Reference 15, and properties for Inconel 617 and Inconel 718 were obtained from Reference 16. Material properties for the Saffil fibrous insulation layer were obtained from Reference 6. Weights for the "box beam", "compliant support", and "compliant sides" components represent nominal weights.

Component and total TPS weights for each case are summarized in Table VI. There is a 13% decrease in TPS panel weight between Cases 1 and 2, due to the decreased insulation requirements at STA 802. Case 3 uses Ti 1100 instead of Inconel 617 for the honeycomb sandwich as well as "compliant support" and "compliant sides" components, resulting in a 19% weight reduction. The reduced weight of the honeycomb sandwich contributes to 58% of this weight reduction, with the reduced weight of the "compliant support" and "compliant sides" components contributing to 38% of the weight reduction. It is obvious that titanium is preferable at STA 802 if the outer surface can be made to withstand the 1225 °F reentry temperature. The severe acoustic pressure and thermal gradients resulting from increasing honeycomb thickness result in a 49% increase in honeycomb sandwich weight at STA 1200 (Case 4). Changes in other component weights are minimal and overall TPS weight is increased by 18%.

Conclusions

Thermal sensitivity studies were performed to determine the influence of analysis and design parameters on insulation sizing. It was found that groundhold purging at –160 °F will increase cryogenic insulation requirements at some vehicle stations. If possible the purge temperature should be lowered. In addition, performing reentry purging was not effective in reducing insulation requirements for the initiation times examined. It is possible that purging at supersonic velocity would be beneficial. Initial temperature of the TPS and tank on reentry has a large effect on insulation sizing, with initial temperatures greater than 70 °F resulting in significant insulation weight penalties. Finally, it was seen that in general increasing the TPSS temperature limit did not significantly reduce TPS weight when tank structure is a epoxy composite.

A sizing process was created for metallic TPS panels using a coupled thermal and structural analysis approach. The process included insulation sizing using the thermal model generated for the sensitivity studies, deflection analysis of the outer honeycomb sandwich panel using a linear static finite element model, and local failure analysis of the honeycomb panel using Hypersizer. Sizing was performed at vehicle stations 240, 802 and 1200 along the windward centerline of a

lifting body RLV. In all cases, the Saffil fibrous insulation layer was sized during reentry by the temperature limit of the TPSS. The cryogenic-foam-filled honeycomb core tank wall was sized either by structural loading, using results from Reference 7, or the constraint on heat flux into the tank during groundhold. At STA 240, near the nose of the RLV, the TPS outer honeycomb sandwich panel was sized by maximum aerodynamic pressure during ascent. At STA 802 the panel was sized by acoustic loading during liftoff. Finally, at STA 1200 the panel was sized by a combination of acoustic loading during liftoff and thermal gradient induced deflection during reentry. In all cases, the critical local failure mode of the honeycomb sandwich was intracell dimpling of the facesheets.

TPS panel weight decreased from STA 240 to STA 802 due to decreased insulation requirements. If Ti 1100 can be used at temperatures of 1225 °F, a significant weight savings can be realized in the region of STA 802. Finally, TPS panel weight increases at STA 1200 due to acoustic pressure and thermal gradients resulting from increased honeycomb thickness.

References

[1]Poteet, C. C.; Blosser, M. L.: Improving Metallic Thermal Protection System Hypervelocity Impact Resistance Through Design of Experiments Approach. To be presented at the 40th Aerospace Sciences Meeting and Exhibit, January 14 – 17, 2002/ Reno NV. Available as AIAA-2002-0912.

[2]Dorsey, J. T.; Chen, R.; and Poteet, C. C.: Metallic Thermal Protection System Technology Development: Concepts, Requirements and Assessment Overview. To be presented at the 40th Aerospace Sciences Meeting and Exhibit, January 14 – 17, 2002/ Reno NV. Available as AIAA-2002-0502.

[3]Blosser, M. L.; Chen, R.; Schmidt, I.; Dorsey, J.T.; Poteet, C. C.; Daryabeigi, K.; and Bird, K.: Advanced Metallic Thermal Protection System Development. To be presented at the 40th Aerospace Sciences Meeting and Exhibit, January 14 – 17, 2002/ Reno NV. Available as AIAA-2002-0504.

[4]Chen, R.; Blosser, M. L.: Metallic TPS Panel Flutter Study. To be presented at the 40th Aerospace Sciences Meeting and Exhibit, January 14 – 17, 2002/ Reno NV. Available as AIAA-2002-0501.

[5]Blosser, M. L.: Investigation of Fundamental Modeling and Thermal Performance Issues for a Metallic TPS Design. To be presented at the 40th Aerospace Sciences Meeting and Exhibit, January 14-17, 2002/ Reno NV. Available as AIAA-2002-0503.

[6]Blair, W.; Meaney, J. E.; and Rosenthal, H. A.: *Re-Design of Titanium Multi-Wall Thermal Protection System Test Panels.* NASA CR-172247, 1984.

[7]Wang, J. T.; et. al.: Cryogenic Tank Structure Sizing with Structural Optimization Method. Presented at 42nd AIAA / ASME / ASCE / AHS / ASC Structures, Structural Dynamics, and Materials Conference, April 16 – 19, 2001/ Seattle, WA. Available as AIAA-2001-1599.

[8]Blosser, M. L.," Advanced Metallic Thermal Protection Systems for Reusable Launch Vehicles," Ph.D. Dissertation, University of Virginia, May, 2000.

[9]Kennard, E. H.: *Kinetic Theory of Gases,* McGraw – Hill, New York, 1938.

[10]Swann, R. T., and Pittman, C. M., "Analysis of Effective Thermal Conductivites of Honeycomb-Core and Corrugated-Core Sandwich Panels," NASA TN D-714, April, 1961.

[11]Poteet, C. C., "Groundhold and Reentry Purge Parameter Trade Study," Lockheed Martin, Langley Program Office, Hampton, VA, LMES SDSR 99-01, 1999.

[12]Hypersizer Analytical Methods & Verification Examples, 3rd Edition, Collier Research Corporation, Unpublished, 1999, available at collier-research.com.

[13]Gruszczynski, M. J., Thorp, V. L., Heim, W. J., and Swanson, N. J.: Design, Development, and Test of the Atlas Liquid Hydrogen Propellant Tank Foam Insulation System. Proceedings from AIAA 26th Thermophysics Conference. AIAA Paper 91-1438, 1991.

[14]Weiser,E. S.; et. al.: Polyimide foams for aerospace vehicles. High Perform. Polym. **12** (2000) 1-12. Printed in the UK.

[15]Hutt, A. J.; Parris, W. M.: "TIMETAL-1100 Sheet Properties", Titanium '92 Science and Technology, The Minerals, Metals and Materials Society, 1993.

[16]Brown, W. F.; Mindlin, H.; and Ho, C. Y.: Aerospace Structural Metals Handbook, CINDA/USAF CRDA Handbooks Operation, Purdue Univ., 1994.

Table I: Representative Loads Table at STA 1200" along the RLV windward centerline

TPS Loads, RLV 3c, Ti 1100 TPS at 1200" Windward Centerline
Iteration 3

File Sources:		**Misc Info:**		
Analysis Date	2/28/2001	Outer Surface Material:	Ti 1100	
This filename	LoadsRLV3c.xls	Max. Surface Temperature (F):	1139.767	
Ascent_performance_trajectory	rlv3c_nom_ascent.xls 1	Duration above 1100 F (s):	720	
Ascent_heating_trajectory	all_asc_wind.xls	Honeycomb Thickness(in):	0.7	
Ascent_time_vs_temperature	l3Case4-1	Honeycomb Cell Parameters:	1/4" square, 2 mil gage	
Entry_performance_trajectory	rlv3c_nom_entry.xls 1	Facesheet Thickness(in):	0.008	Sized by:
Entry_heating_trajectory	all_rent_wind.xls	Insulation Thickness (in):	1.86	Support
Entry_time_vs_temperature	l3Case4-7	Foam Thickness(in):	0.82	Structure Min

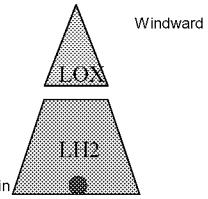

trajectory_phase		Liftoff	ascent max Fn	ascent max delta P	ascent abs(max T1-T2)	ascent max ax	entry abs(max T1-T2)	entry max qdot	entry max delta P
Parameter	unit								
time	sec	6	52	45	130	126	2275	485	1870
mach	-	0.05	0.79	0.68	4.20	4.20	1.10	26.90	6.75
Pstatic	psia	1.46E+01	6.90E+00	8.54E+00	9.10E-02	9.10E-02	3.43E+00	3.82E-02	3.06E-01
Patm	psia	1.46E+01	6.85E+00	8.47E+00	9.10E-02	9.10E-02	3.31E+00	9.30E-05	3.10E-02
T1	F	60	43	44	285	272	71	1037	1035
T2	F	47	43	44	84	76	427	855	690
Tbbeam_top	F	-100	-98	-98	-94	-94	316	106	267
Tbbeam_bottom	F	-106	-99	-100	-95	-95	315	80	261
Ttpss_top	F	-107	-106	-106	-102	-102	286	74	218
Ttpss_mid	F	-112	-112	-112	-113	-113	207	71	142
Ttpss_bot	F	-115	-121	-120	-129	-128	255	72	182
Ttank_outer	F	-115	-121	-120	-129	-128	255	72	182
Ttank_inner	F	-417	-418	-418	-418	-418	120	70	91
vehicle_ax	G's	1.38E+00	1.55E+00	1.59E+00	3.00E+00	3.00E+00	?	-1.50E-02	-0.3944
vehicle_ay	G's	0.00E+00	0.00E+00	0.00E+00	0.00E+00	0.00E+00	?	0.00E+00	0
vehicle_az	G's	6.10E-04	-6.60E-02	-1.63E-02	6.10E-02	6.10E-02	?	-1.70E-01	-1.646
Delta p (aero)	psia	6.95E-03	4.60E-02	7.00E-02	0.00E+00	0.00E+00	1.24E-01	3.81E-02	2.75E-01
Delta p(aero - modified)	psia	5.80E-02	3.84E-01	5.84E-01	0.00E+00	0.00E+00	1.24E-01	3.81E-02	2.75E-01
Delta p(accoustic)	psia	9.94E-01	2.96E-02	2.44E-02	9.90E-03	9.90E-03	1.23E-02	4.26E-04	8.68E-03
Delta Pult+	psia	4.26E+00	6.62E-01	9.21E-01	4.16E-02	4.16E-02	2.26E-01	5.51E-02	4.21E-01
Delta Pult-	psia	-4.09E+00	-4.13E-01	-7.16E-01	-4.16E-02	-4.16E-02	-1.22E-01	-5.16E-02	-3.48E-01

Table II: Transition Based Deflection Limits, from Reference 2.

Location	Deflection/L
Leading Edge	0.01
Windward Forebody	0.01
Windward Aft Body	0.015
Leeward Forebody	0.015
Leeward Aft Body	0.025

Table III: Insulation Sizing Summary

Case Number	Vehicle Station	Max. Surface Temp. (F)	Reentry Insulation Thickness (in)	Sized by	Cryo Insulation Thickness (in)	Sized by
1	240	1514	3.08	TPS Support	0.646	Min. Thickness
2	802	1225	2.10	TPS Support	0.62	Heat Flow
3	802	1224	1.98	TPS Support	0.62	Heat Flow
4	1200	1140	1.89	TPS Support	0.82	Min. Thickness

Table IV: Structural Sizing Summary

		Honeycomb Properties:				***Facesheet Properties:***		***Sizing Information:***		
Case Number	Vehicle Station	Material	Thickness (in)	Cell Size (in)	Gauge (in)	Material	Thickness (in)	Critical Deflection Loadcase	Critical Local Failure Loadcase	Critical Local Failure Mode
1	240	Inconel	0.35	0.25	0.002	Inconel	0.006	Ascent, max ΔP	Ascent, max ΔP	Intracell dimpling
2	802	Inconel	0.30	0.25	0.002	Inconel	0.006	Liftoff	Liftoff	Intracell dimpling
3	802	Titanium	0.45	0.25	0.002	Titanium	0.006	Liftoff	Liftoff	Intracell dimpling
4	1200	Titanium	0.75	0.25	0.002	Titanium	0.008	Entry, max ΔT	Liftoff	Intracell dimpling

Table V: Representative TPS Panel Weights Calculation, STA 1200

Material Properties:		**Weights (lb)**	**Part Weight**	**Quantity**	**Total Part Weight**	**Component Weight**
Titanium density (lb/in3):	0.16	***Honeycomb Sandwich***				1.97
Saffil density (lb/in3):	0.0017	-outer skin	0.41	1	0.41	
Ti h/c core density (%):	1.63	-inner skin	0.40	1	0.40	
Ti h/c Lid density (lb/in3):	0.32	- braze alloy	0.04	1	0.04	
		- core	1.13	1	1.13	
		Reentry Insulation				0.98
		-Saffil	0.98	1	0.98	
Parameters (in):		***Box Beam***				0.42
Repeat Length:	18.00	-Hat Section	0.20	1	0.20	
Length of Side:	17.50	-Base Frame Closure	0.14	1	0.14	
Height of Side Closure:	2.64	-Bottom Closure	0.08	1	0.08	
Side Closure Thickness:	0.003	***Compliant Support***				0.50
Outer H/C Core Thickness:	0.75	-Upper Corner	0.05	4	0.19	
Outer Facesheet Thickness:	0.008	-Hole Plug	0.02	4	0.06	
Inner Facesheet Thickness:	0.008	-Bellows	0.01	4	0.05	
Overhanging Lip:	0.315	-Standoff	0.01	4	0.04	
Insulation Thickness:	1.89	-Lower Corner	0.04	4	0.15	
Box Beam Height:	0.50	***Compliant Sides***				0.09
Box Beam Top Width:	0.50	-Side Closure	0.02	4	0.09	
Ti. LID layer thickness:	0.0002	***Total Weight***				3.96

Table VI: Component and Total Weight Variation with Vehicle Station

		Component Weights (lb):					***TPS Panel:***	
Case Number	Vehicle Station	Honeycomb	Reentry Insulation	Box Beam	Compliant Supports	Compliant Sides	Weight (lb)	Areal Density (lb/ft2)
1	240	1.99	1.61	0.42	0.82	0.22	5.05	2.24
2	802	1.92	1.09	0.42	0.82	0.15	4.39	1.95
3	802	1.32	1.02	0.42	0.50	0.08	3.35	1.49
4	1200	1.97	0.98	0.42	0.50	0.09	3.96	1.76

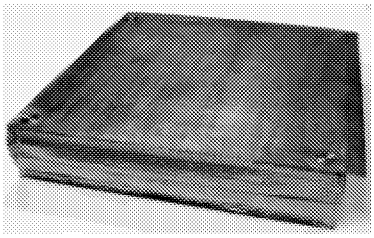

Fabricated Panel

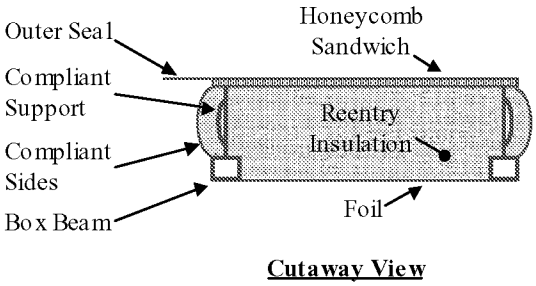

Cutaway View

Figure 1. As fabricated and cutaway schematic views of ARMOR TPS.

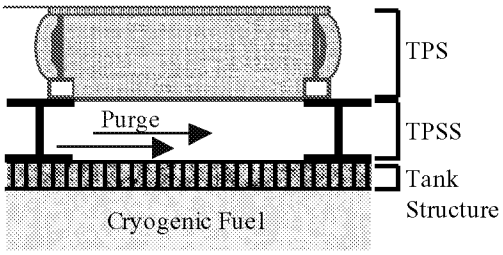

Figure 3. Cutaway schematic view of TPS mounted on TPSS and tank.

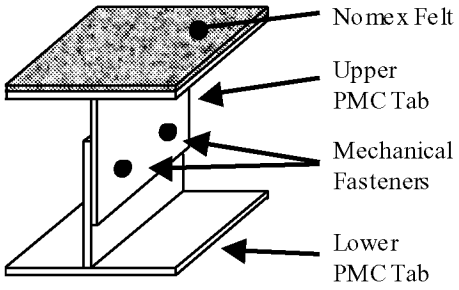

Figure 4. Schematic of TPSS

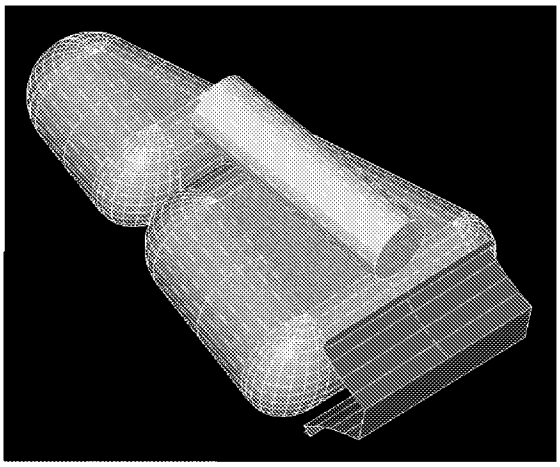

Figure 2. RLV 3C semi-conformal cryogenic fuel tanks

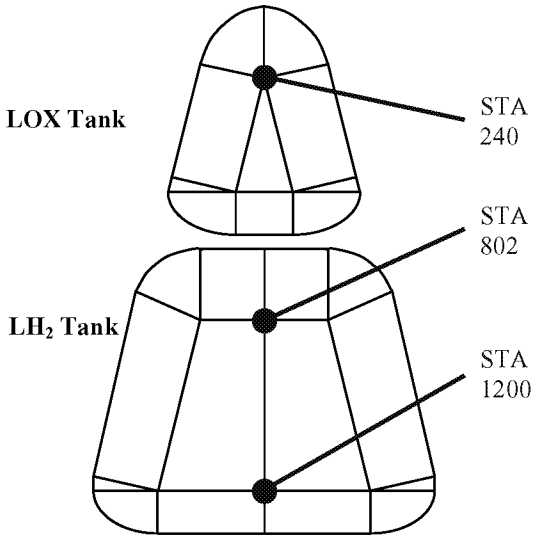

Figure 5. Location of vehicle stations studied relative to cryogenic fuel tanks.

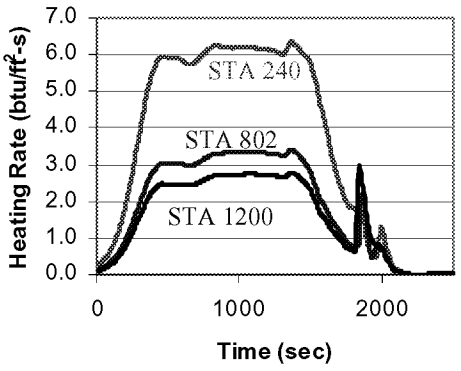

Figure 6. Heating rates at the three body points investigated.

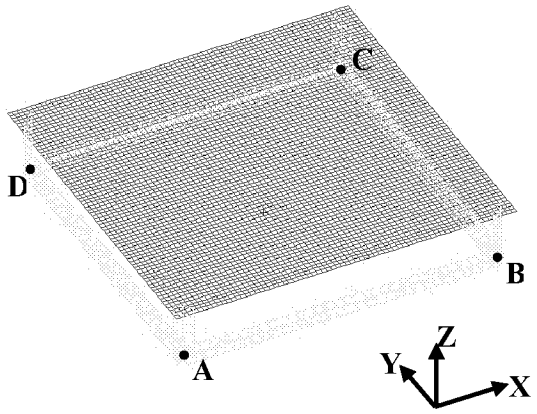

Figure 8. TPS Panel Model used in linear static analysis. Constraints A, B, C, and D described in text.

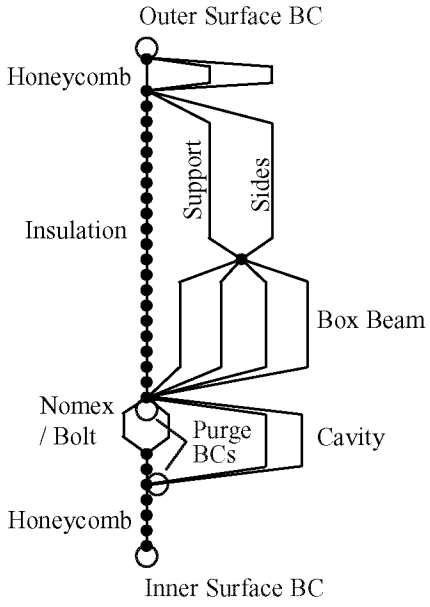

Figure 7. Thermal Finite Element Model of TPS/TPSS/Tank System. Refer to Figure 3 for schematic of system.

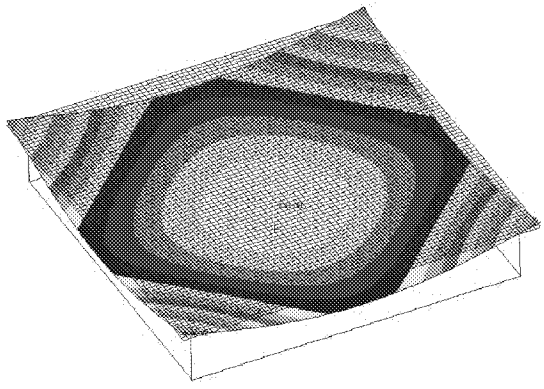

Figure 9. Z displacement due to positive (inward) external pressure.

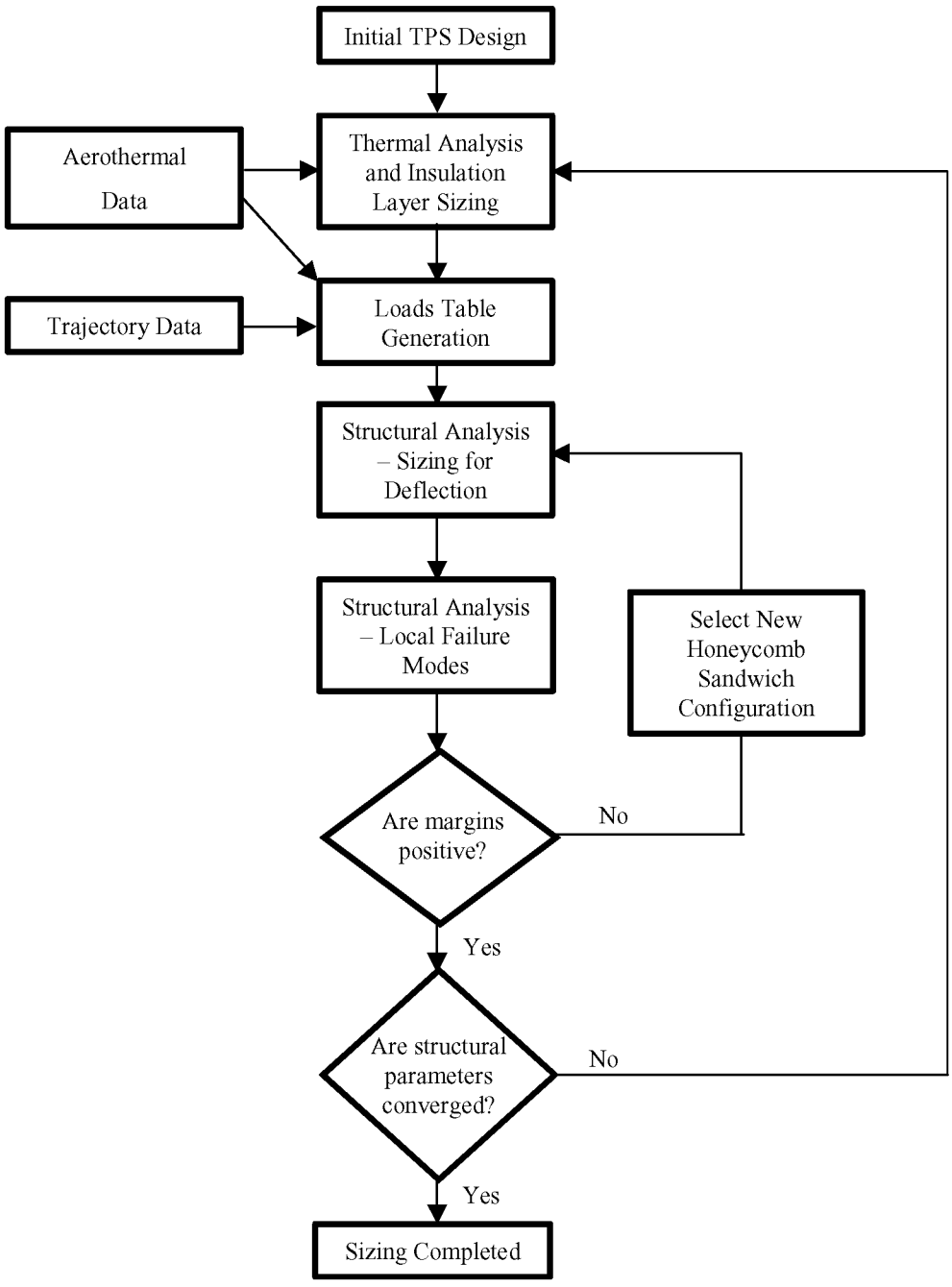

Figure 10. Thermal-Mechanical Sizing Process

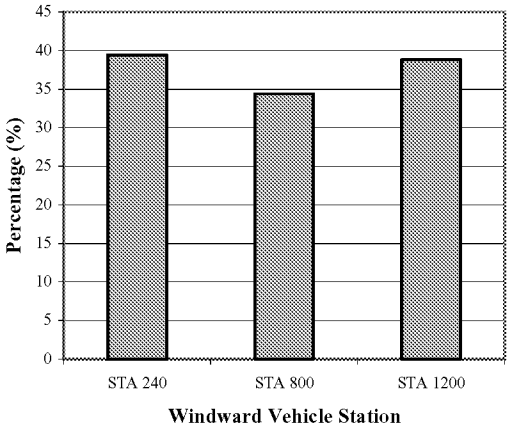

Figure 11. Percentage of TPS/Tank weight directly influenced by insulation thickness.

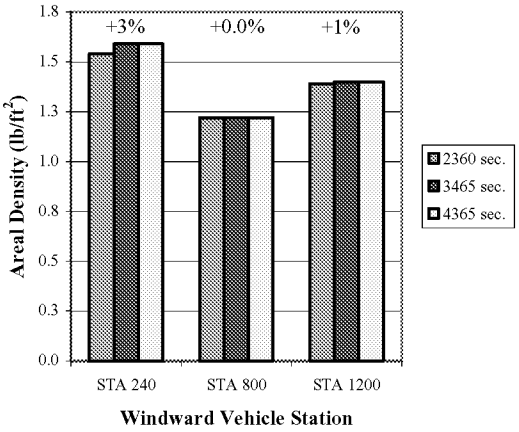

Figure 13. Effect of early reentry purge on Insulation Related TPS/Tank weight. Percentages list maximum difference in Areal Density for three reentry purge initiation times.

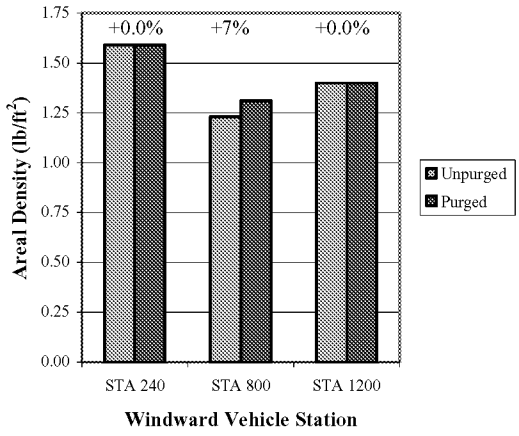

Figure 12. Comparison of Insulation Related Weight of Unpurged vs. Purged Systems. Percentages list difference in Areal Density between systems purged and unpurged during groundhold.

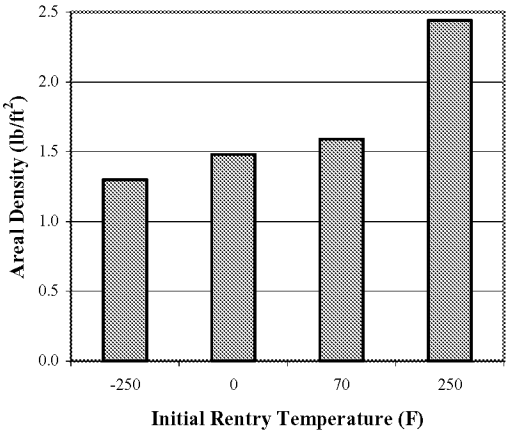

Figure 14. Effect of assumed initial reentry temperature on Insulation Related TPS/Tank weight.